

Quasi-hierarchical Powell-Sabin B-splines

Hendrik Speleers

Paul Dierckx

Stefan Vandewalle

Report TW 472, October 2006



Katholieke Universiteit Leuven
Department of Computer Science
Celestijnenlaan 200A – B-3001 Heverlee (Belgium)

Quasi-hierarchical Powell-Sabin B-splines

Hendrik Speleers

Paul Dierckx

Stefan Vandewalle

Report TW 472, October 2006

Department of Computer Science, K.U.Leuven

Abstract

Hierarchical Powell-Sabin splines are C^1 -continuous piecewise quadratic polynomials defined on a hierarchical triangulation. The mesh is obtained by partitioning an initial conforming triangulation locally with a triadic split, so that it is no longer conforming. We propose a normalized quasi-hierarchical basis for this spline space. The B-spline basis functions have a local support, they form a convex partition of unity, they are stable, and they admit local subdivision. We consider two applications: data fitting and surface modelling.

Keywords : Powell-Sabin splines, quasi-hierarchical splines, normalized basis, adaptive mesh refinement

AMS(MOS) Classification : Primary : 65D07, Secondary : 65D17, 68U07

Quasi-hierarchical Powell-Sabin B-splines

Hendrik Speleers, Paul Dierckx and Stefan Vandewalle

*Department of Computer Science, Katholieke Universiteit Leuven
Celestijnenlaan 200A, B-3001 Leuven, Belgium*

Abstract

Hierarchical Powell-Sabin splines are C^1 -continuous piecewise quadratic polynomials defined on a hierarchical triangulation. The mesh is obtained by partitioning an initial conforming triangulation locally with a triadic split, so that it is no longer conforming. We propose a normalized quasi-hierarchical basis for this spline space. The B-spline basis functions have a local support, they form a convex partition of unity, they are stable, and they admit local subdivision. We consider two applications: data fitting and surface modelling.

Keywords: Powell-Sabin splines, quasi-hierarchical splines, normalized basis, adaptive mesh refinement

AMS classification: 65D07, 65D17, 68U07

1 Introduction

The flexibility of geometric modelling of complex surfaces relies crucially on the use of an appropriate mathematical representation [9]. Typically one wants to represent the surface s as a linear combination of basis functions ϕ_i ,

$$s = \sum_{i=1}^N c_i \phi_i. \quad (1.1)$$

The surface can be locally controlled and edited in a predictable way when the basis functions satisfy certain properties. Particularly important are the properties of having a local support, and forming a convex partition of unity, i.e.,

$$\phi_i \geq 0, \quad \text{and} \quad \sum_{i=1}^N \phi_i = 1, \quad (1.2)$$

In order to generate sufficiently smooth surfaces, continuity conditions can be imposed.

Commonly used in many computer aided geometric design (CAGD) packages are basis functions of tensor product B-spline type [5]. A drawback, however, is that such splines are restricted to regular rectangular meshes. As a consequence, a single vertex cannot be inserted in such a mesh without propagating an entire row or column of vertices. This often rules out an adequate adaptive mesh refinement. The local refinement of spline surfaces was pioneered by Forsey and Bartels [10, 11] in their study of hierarchical tensor product B-splines. These so-called H-splines can be locally adapted by using overlays: a local fine spline is put on top of a given coarse spline. Based on this model, they were able to create complex surfaces economically. Kraft [14] developed a compact basis for this hierarchical spline space.

In a more general framework, Grinspun *et al.* [12, 15] focused on conforming hierarchical adaptive refinement methods (CHARMS). They outlined two kinds of adaptive space refinement strategies,

leading to *hierarchical* and *quasi-hierarchical* bases for refined spaces. In the former case, the basis functions of the original (coarse) space are retained in the basis of the refined space. The extra basis functions therefore represent the finer details added onto the coarser approximation scales. Examples of bases constructed in this way are the classical hierarchical bases studied in the finite element literature (see, e.g., [27]), and the wavelet bases [13], widely used in signal analysis and image processing. In a quasi-hierarchical refinement method, the coarse-level basis functions are replaced by finer-level basis functions. The finer functions are related to the coarser functions by subdivision. Because of the generation of nested spaces in the CHARMS methodology, one can easily incorporate multigrid solvers [27, 2].

Other spline spaces built on non-conforming meshes involve no notion of hierarchy. Weller and Hagen [25] studied spaces of piecewise polynomials with an irregular, locally refineable knot structure. Their approach is restricted to so-called semi-regular basis functions. Sederberg *et al.* developed T-splines [20, 19]. These splines are defined over T-meshes, which are formed by a set of horizontal and vertical line segments where T-junctions are allowed. Deng *et al.* recently presented other splines on T-meshes in [4].

In this paper, we consider a new type of quasi-hierarchical basis functions, which we shall call quasi-hierarchical Powell-Sabin (QHPS) B-splines. They form a compact basis for the hierarchical Powell-Sabin spline space, i.e., a C^1 -continuous bivariate quadratic spline space defined on a particular hierarchical triangulation. The mesh is obtained by refining an initial conforming triangulation by (local) triadic splits. Using the subdivision rules for the classical Powell-Sabin splines [24], the C^1 -continuity constraints between neighbouring triangles on different refinement levels can be determined easily, efficiently and in a stable way. This allows us to construct an inherently C^1 -continuous normalized spline basis on the hierarchical mesh. The resulting basis functions satisfy the same interesting properties as the classical Powell-Sabin B-splines [6]: they have a local support, they form a convex partition of unity (1.2), and they can be geometrically interpreted by means of tangent control triangles. In addition, the hierarchical mesh admits local subdivision in a very straightforward way. That is an advantage over classical Powell-Sabin splines. There, the necessary conformity of the mesh requires specialized shape-improvement and refinement propagation techniques [21] to adopt local subdivision. The QHPS idea can be further extended to parametric surfaces.

The paper is organized as follows. Section 2 recalls the definition of the Powell-Sabin spline space, and covers the relevant aspects of the Powell-Sabin subdivision scheme. In section 3 the hierarchical Powell-Sabin spline space is defined, and the construction of a suitable normalized quasi-hierarchical basis is presented. In section 4 we discuss some practical implementation issues. Section 5 illustrates the power of the quasi-hierarchical spline representation with some applications. Finally, in section 6 we end with some concluding remarks.

2 Powell-Sabin splines

2.1 The space of Powell-Sabin splines

Consider a simply connected subset $\Omega \subset \mathbb{R}^2$ with polygonal boundary $\partial\Omega$. Assume a conforming triangulation Δ of Ω is given, consisting of t triangles $\rho_j, j = 1, \dots, t$, and having n vertices $V_k, k = 1, \dots, n$. A triangulation is conforming if no triangle contains a vertex different from its own three vertices.

The Powell-Sabin (PS) refinement Δ^* of Δ partitions each triangle ρ_j into six smaller triangles with a common vertex Z_j . This partition is defined algorithmically as follows:

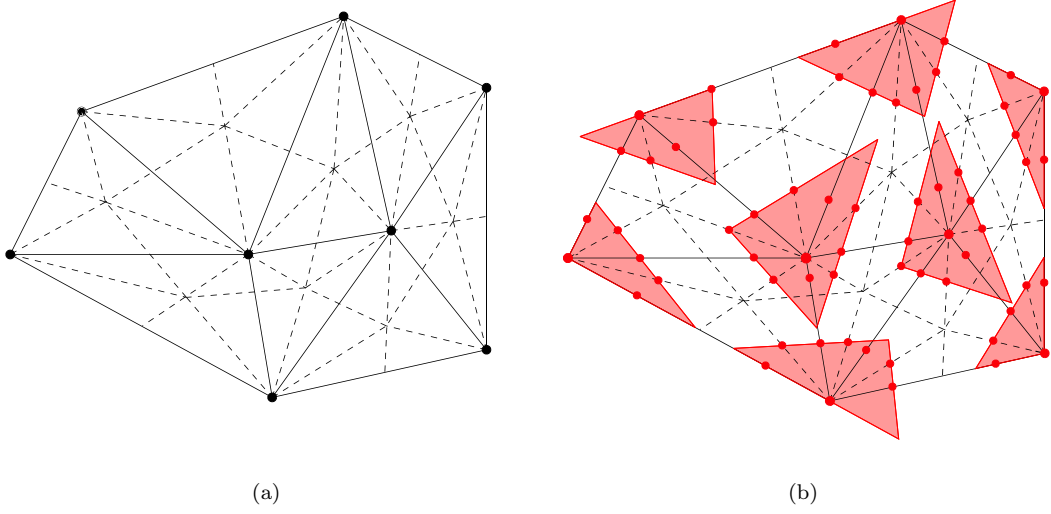


Figure 1: (a) A PS refinement Δ^* (dashed lines) of a given triangulation Δ (solid lines); (b) the PS points (bullets) and a set of suitable PS triangles (shaded).

Definition 2.1 (PS refinement).

1. Choose an interior point Z_j in each triangle ρ_j . If two triangles ρ_i and ρ_j have a common edge, then the line joining Z_i and Z_j should intersect the common edge at some point R_{ij} .
2. Join each point Z_j to the vertices of ρ_j .
3. For each edge of the triangle ρ_j
 - (a) which is common to a triangle ρ_i : join Z_j to R_{ij} ;
 - (b) which belongs to the boundary $\partial\Omega$: join Z_j to an arbitrary point R_j on that edge.

In Figure 1(a) such a PS refinement of a given triangulation is drawn in dashed lines. Let Π_2 be the space of bivariate polynomials of degree 2. The space of piecewise quadratic polynomials on Δ^* with global C^1 -continuity is called the Powell-Sabin spline space:

$$S_2^1(\Delta^*) = \left\{ s \in C^1(\Omega) : s|_{\rho_j^*} \in \Pi_2, \rho_j^* \in \Delta^* \right\}. \quad (2.1)$$

Powell and Sabin [18] proved that the following interpolation problem

$$s(V_k) = f_k, \quad \frac{\partial s}{\partial x}(V_k) = f_{x,k}, \quad \frac{\partial s}{\partial y}(V_k) = f_{y,k}, \quad k = 1, \dots, n, \quad (2.2)$$

has a unique solution $s(x, y) \in S_2^1(\Delta^*)$ for any given set of n $(f_k, f_{x,k}, f_{y,k})$ -values. It follows that the dimension of the Powell-Sabin spline space $S_2^1(\Delta^*)$ is equal to $3n$. Every Powell-Sabin spline can be represented as a linear combination of $3n$ basis functions,

$$s(x, y) = \sum_{i=1}^n \sum_{j=1}^3 c_{i,j} B_i^j(x, y). \quad (2.3)$$

To construct the basis functions $B_i^j(x, y)$ we use a geometric method suggested by Dierckx [6]. For each vertex V_i this approach constructs a PS triangle $t_i(Q_{i,1}, Q_{i,2}, Q_{i,3})$. This triangle must

contain the so-called PS points. The vertex itself is a PS point, together with the midpoints of all edges in the PS refinement Δ^* containing V_i . Figure 1(b) shows the PS points and a set of suitable PS triangles. From such a PS triangle with corners $Q_{i,j}(X_{i,j}, Y_{i,j})$, $j = 1, 2, 3$, one can uniquely determine the values $(\alpha_{i,j})$, and the x - and y -derivatives $(\beta_{i,j}, \gamma_{i,j})$ of the three B-splines $B_i^j(x, y)$ at the vertex $V_i(x_i, y_i)$ as

$$\begin{bmatrix} \alpha_{i,1} & \alpha_{i,2} & \alpha_{i,3} \\ \beta_{i,1} & \beta_{i,2} & \beta_{i,3} \\ \gamma_{i,1} & \gamma_{i,2} & \gamma_{i,3} \end{bmatrix} \begin{bmatrix} X_{i,1} & Y_{i,1} & 1 \\ X_{i,2} & Y_{i,2} & 1 \\ X_{i,3} & Y_{i,3} & 1 \end{bmatrix} = \begin{bmatrix} x_i & y_i & 1 \\ 1 & 0 & 0 \\ 0 & 1 & 0 \end{bmatrix}. \quad (2.4)$$

The value and derivatives of $B_i^j(x, y)$ at the other vertices are chosen to be zero, such that the basis functions are uniquely defined by the interpolation problem (2.2). Since these PS B-splines are quadratic polynomials on each triangle in Δ^* , they can be represented in a Bernstein-Bézier formulation by means of Bézier ordinates [8]. In [6] it is shown how the values of these Bézier ordinates can be derived in a stable way. In the Bernstein-Bézier representation the Powell-Sabin splines can be easily represented, evaluated, manipulated and displayed using the de Casteljau algorithm.

The Powell-Sabin B-splines have a local support: $B_i^j(x, y)$ vanishes outside the molecule of vertex V_i . The molecule of a vertex (also called vertex star or 1-ring) is the union of all triangles that contain the vertex. Dierckx showed in [6] that the proposed basis $\mathcal{B} = \{B_i^j(x, y)\}$ forms a convex partition of unity (1.2). Furthermore, Maes *et al.* [17] proved that \mathcal{B} is an L_∞ -stable basis. For the max-norms

$$\|c\|_\infty = \max_{i,j} |c_{i,j}|, \quad \text{and} \quad \|s(x, y)\|_\infty = \max_{\Omega} |s(x, y)|, \quad (2.5)$$

they showed that for all choices of the coefficient vector c , one has that

$$k_1 \|c\|_\infty \leq \|s(x, y)\|_\infty \leq k_2 \|c\|_\infty, \quad (2.6)$$

where $k_2 = 1$, and k_1 depends only on the smallest angle θ_Δ in the triangulation Δ and on the size of the PS triangles. Moreover, the smaller the PS triangles the better (the larger) the approximation constant. Stable bases for higher order spline spaces on Powell-Sabin splits are developed in [1, 16].

We define the PS control points as

$$C_{i,j} = (Q_{i,j}, c_{i,j}). \quad (2.7)$$

These points define PS control triangles $T_i(C_{i,1}, C_{i,2}, C_{i,3})$, which are tangent to the spline surface $z = s(x, y)$ at the vertices V_i . The projection of the control triangles T_i in the (x, y) -plane are the PS triangles t_i .

The above properties are the heart of the computational effectiveness of Powell-Sabin splines in many application domains, see [7, 23, 22].

2.2 Powell-Sabin spline subdivision

Subdivision is a procedure to represent a surface on a finer mesh than the mesh on which it is originally defined. The subdivision scheme for Powell-Sabin splines developed in [24, 21] is based on the so-called $\sqrt{3}$ -refinement scheme, illustrated in Figure 2. The refined triangulation, which we shall denote as $\Delta^{\sqrt{3}}$, is constructed by inserting a new vertex V_{ijk} at the position of the interior point Z_{ijk} inside each triangle $\rho(V_i, V_j, V_k)$. The edges of the original PS refinement Δ^* that are not edges in the original triangulation Δ form the edges of the new triangulation $\Delta^{\sqrt{3}}$. The interior points of the new PS refinement are chosen on the edges of Δ . Then, the edges of Δ will be a subset of the edges of the new PS refinement. Applying the $\sqrt{3}$ -refinement scheme twice, we obtain a triadic split, as shown in Figure 2. Every original edge is trisected and each original triangle is split into nine subtriangles.

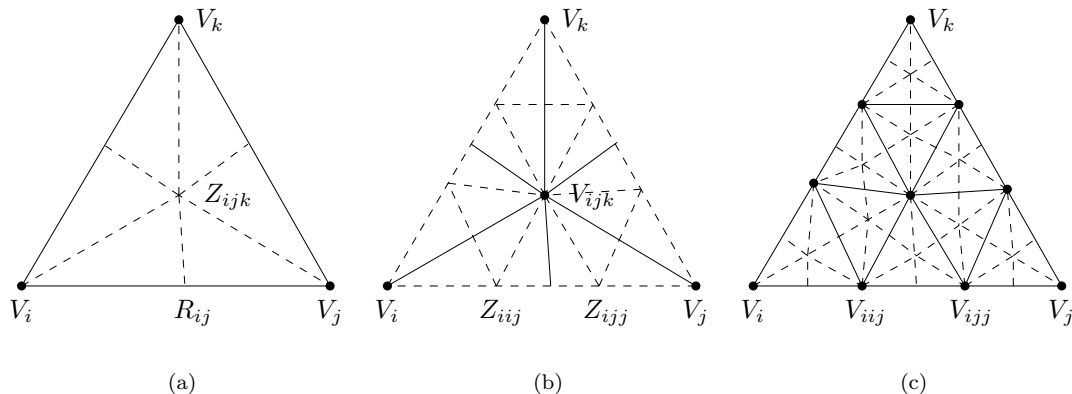


Figure 2: Two successive $\sqrt{3}$ -refinement steps result in a triadic split. The corresponding PS refinement is indicated with dashed lines.

The corresponding Powell-Sabin $\sqrt{3}$ -subdivision rules are described in [24]. These rules learn how to derive the PS control triangles on the refined mesh, from the given PS control triangles on the original mesh. For the original vertices one can reuse the old PS triangles and the corresponding spline coefficients. However, it is also possible to determine a smaller PS triangle by rescaling the original one. The PS triangles $t_{ijk}(Q_{ijk,1}, Q_{ijk,2}, Q_{ijk,3})$ associated with the new vertices V_{ijk} in the refined mesh are defined by

$$Q_{ijk,1} = (V_{ijk} + V_i)/2, \quad Q_{ijk,2} = (V_{ijk} + V_j)/2, \quad \text{and,} \quad Q_{ijk,3} = (V_{ijk} + V_k)/2. \quad (2.8)$$

The corresponding coefficients are computed as convex combinations

$$c_{ijk,1} = \tilde{L}_{i,1}c_{i,1} + \tilde{L}_{i,2}c_{i,2} + \tilde{L}_{i,3}c_{i,3}, \quad (2.9a)$$

$$c_{ijk,2} = \tilde{L}_{j,1}c_{j,1} + \tilde{L}_{j,2}c_{j,2} + \tilde{L}_{j,3}c_{j,3}, \quad (2.9b)$$

$$c_{ijk,3} = \tilde{L}_{k,1}c_{k,1} + \tilde{L}_{k,2}c_{k,2} + \tilde{L}_{k,3}c_{k,3}. \quad (2.9c)$$

The triplets $(\tilde{L}_{i,1}, \tilde{L}_{i,2}, \tilde{L}_{i,3})$, $(\tilde{L}_{j,1}, \tilde{L}_{j,2}, \tilde{L}_{j,3})$ and $(\tilde{L}_{k,1}, \tilde{L}_{k,2}, \tilde{L}_{k,3})$ are the barycentric coordinates of $Q_{ijk,1}$, $Q_{ijk,2}$, and $Q_{ijk,3}$ respectively with respect to the PS triangles of the surrounding vertices V_i , V_j and V_k . Since these points lie inside the corresponding PS triangles, all weights are positive. Applying those rules twice, one obtains the control triangles of the new vertices in a triadically refined mesh, e.g., of vertices V_{ijj} and V_{ijj} in Figure 2(c). Adapted subdivision rules are needed for vertices at the boundary of the domain, see [24, 21]. Figure 3 illustrates the triadic subdivision for a given PS spline.

3 Hierarchical Powell-Sabin splines

When an increased resolution is only required in a small part of a surface, the use of global subdivision may lead to excessive computational and storage costs. In such case, a local adaptive subdivision strategy is recommended. The $\sqrt{3}$ -subdivision scheme can be used to refine a mesh locally. In order to avoid poorly shaped triangles a refinement propagation is proposed in [21]. This improves the shape of the triangles near the boundary of the refinement region. The use of such specialized shape-improvement heuristics and the propagation of the refinement into regions where the refinement is not strictly required, could be avoided if non-conforming triangulations were allowed. In this paper, we will show how classical PS splines can be adapted towards certain non-conforming triangulations.

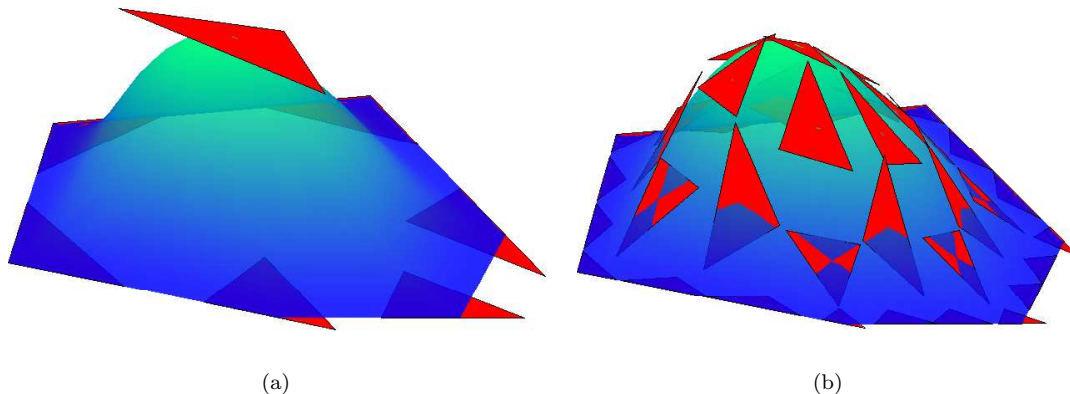


Figure 3: (a) A PS spline with 7 control triangles; (b) the triadically subdivided spline.

3.1 Construction of a hierarchical Powell-Sabin spline space

We define a hierarchical triangulation or mesh Δ_H on Ω as a set of non-overlapping triangles that partition the domain Ω . It is constructed from an initial conforming triangulation Δ^0 on Ω by partitioning successively subsets of triangles with a triadic split. The hierarchical triangulation has a total of n vertices. Of these vertices, n_{nc} are non-conforming (or hanging) vertices. They are located on interiors of triangle edges. The remaining ones, i.e. $n_c = n - n_{nc}$, are called conforming vertices. An example of such a mesh is drawn in Figure 4(a) with solid lines. Here, Δ^0 consists of 8 triangles and 8 (conforming) vertices. The hierarchical mesh in the figure consists of 16 triangles and 15 vertices ($n_c = 9$, $n_{nc} = 6$).

To each hierarchical mesh Δ_H we shall associate a hierarchical mesh structure $\mathbf{\Delta}_H$. It is the set of triangles ρ^k that are generated during the construction of Δ_H . The superscript k of a triangle ρ^k refers to the refinement level of that triangle, i.e., the minimal number of refinement steps needed to construct the triangle. The triangles in $\mathbf{\Delta}_H$ that are part of Δ_H are called leaf triangles. We will denote $\mathbf{\Delta}_H^l$ as the subset of $\mathbf{\Delta}_H$ containing all triangles whose level is l or lower, and let Δ_H^l be its corresponding hierarchical triangulation. Note that these mesh structures are nested

$$\Delta^0 \subset \mathbf{\Delta}_H^1 \subset \mathbf{\Delta}_H^2 \subset \dots \subset \mathbf{\Delta}_H. \quad (3.1)$$

A triangulation patch \mathcal{T}^l is defined as the union of connected triangles ρ^l of refinement level l . Such a triangulation patch is a conforming triangulation, on which a classical Powell-Sabin spline can be defined. The triangulation patch of level 0 is equal to Δ^0 . At the other levels, the hierarchical structure $\mathbf{\Delta}_H$ can contain several (local) triangulation patches.

Further on, we shall always assume that Powell-Sabin triadic splits (see Figure 2(c)) are used in the construction of the hierarchical triangulation Δ_H . The PS refinements used in the splitting process generate a particular refinement of Δ_H which partitions each triangle in Δ_H into six subtriangles. We call this refinement the hierarchical Powell-Sabin (HPS) refinement $\mathbf{\Delta}_H^*$ of Δ_H . Analogous to (3.1), the HPS refinement yields a nested structure of sets of triangles

$$\mathbf{\Delta}_H^{*,0} \subset \mathbf{\Delta}_H^{*,1} \subset \mathbf{\Delta}_H^{*,2} \subset \dots \subset \mathbf{\Delta}_H^*. \quad (3.2)$$

In Figure 4(a) such a HPS refinement is drawn in dashed lines. The points R_j at the boundary of each local PS refinement can in principle be chosen freely on the boundary edge. However, we will see in §4.1 that particular choices may simplify the computations.

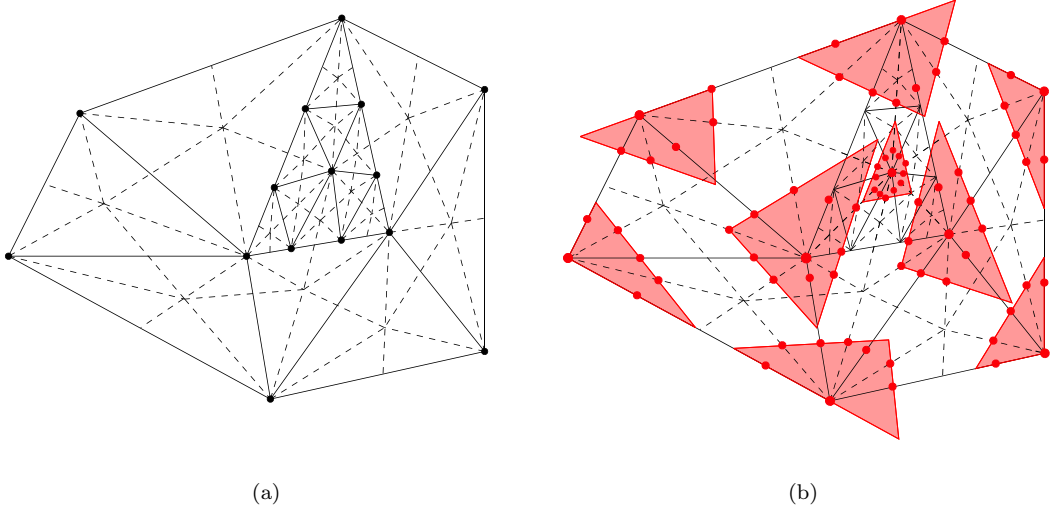


Figure 4: (a) A HPS refinement Δ_H^* (dashed lines) of a given hierarchical triangulation Δ_H (solid lines); (b) the QHPS points (bullets) and a set of suitable QHPS triangles (shaded).

The space of piecewise quadratic polynomials on Δ_H^* with global C^1 -continuity will be called the hierarchical Powell-Sabin spline space:

$$S_{2,H}^1(\Delta_H^*) = \left\{ s_H \in C^1(\Omega) : s_H|_{\rho_j^*} \in \Pi_2, \rho_j^* \in \Delta_H^* \right\}. \quad (3.3)$$

Theorem 3.1 (HPS interpolation). *Given a triplet $(f_k, f_{x,k}, f_{y,k})$ for each conforming vertex V_k in the hierarchical mesh Δ_H , the interpolation problem*

$$s_H(V_k) = f_k, \quad \frac{\partial s_H}{\partial x}(V_k) = f_{x,k}, \quad \frac{\partial s_H}{\partial y}(V_k) = f_{y,k}, \quad (3.4)$$

has a unique solution $s_H(x, y) \in S_{2,H}^1(\Delta_H^*)$.

Proof. From the definitions (2.1) and (3.3) it is easy to see that a HPS spline when restricted on a triangle in Δ_H can be represented by a PS spline. We first show how the n_c triplets $(f_k, f_{x,k}, f_{y,k})$ at the conforming vertices uniquely define a PS spline s_ρ on each triangle $\rho \in \Delta_H$. We then prove that these PS spline patches form a globally C^1 -continuous spline, i.e., the HPS spline s_H .

For all level 0 triangles in Δ_H , which have 3 conforming vertices, the corresponding triplets define a unique PS spline by (2.2). Assume we have already determined the PS splines on the triangles of level $r < l$. The PS splines on the triangles ρ^l are then defined as follows. Using (2.2) and the given triplets $(f_k, f_{x,k}, f_{y,k})$ at the conforming vertices, it is sufficient to show how the value and gradient are determined at the non-conforming vertices of ρ^l . Such a vertex is situated on the interior of an edge of a single triangle ρ^m with $m < l$. Since the corresponding PS spline s_{ρ^m} is already known by assumption, we can use the value and gradient of s_{ρ^m} at the non-conforming vertex. We now prove that this is the only choice that ensures a global C^1 -continuity of the spline patches on Δ_H .

Consider the PS splines s_{ρ^l} and s_{ρ^m} on two neighbouring triangles ρ^l and ρ^m in Δ_H . Suppose that $m \leq l$. We will triadically subdivide s_{ρ^m} ($l - m$) times, such that we obtain a conforming triangulation $\tilde{\Delta}$ on the domain $\rho^l \cup \rho^m$. By (2.2) both PS spline patches form a globally C^1 -continuous quadratic spline on $\tilde{\Delta}$ if and only if they share the same function value and gradient at the two vertices on the common edge. \square

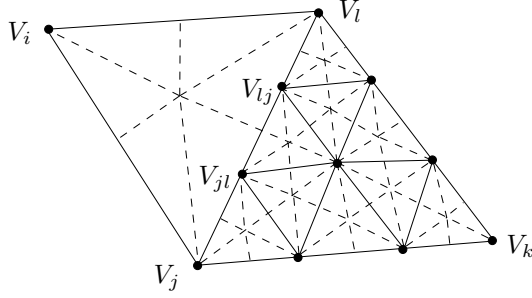


Figure 5: Hierarchical triangular mesh with HPS refinement.

Corollary 3.1 (HPS dimension). *The dimension of $S_{2,H}^1(\Delta_H^*)$ is equal to three times the number of conforming vertices in the hierarchical triangulation.*

Figure 5 displays a hierarchical triangulation with two levels. The mesh contains nine conforming vertices and two non-conforming vertices, i.e. V_{jl} and V_{lj} . The dimension of the HPS spline space on this mesh equals 27.

Remark 3.1. *Let Δ_H be a given hierarchical mesh, and Δ_H^* its HPS refinement, both generated through a local refinement procedure with l refinement levels, starting from the mesh Δ^0 . If instead of a local refinement a global refinement is used in each step, we get a conforming mesh Δ^l and corresponding PS refinement $\Delta^{*,l}$. Assume a consistent selection is made of the new vertices in the local and global refinements, then we have*

$$\Delta_H^* \subseteq \Delta^{*,l}, \quad \text{and} \quad S_{2,H}^1(\Delta_H^*) \subseteq S_2^1(\Delta^{*,l}). \quad (3.5)$$

We shall call $\Delta^{*,l}$ the extended PS refinement of Δ_H^* . Hence, every HPS spline $s_H(x,y)$ can be represented as a Powell-Sabin spline $s^l(x,y)$ on $\Delta^{*,l}$. Let n_l be the number of vertices in Δ^l , then

$$s_H(x,y) = s^l(x,y) = \sum_{i=1}^{n_l} \sum_{j=1}^3 c_{i,j}^l B_i^{j,l}(x,y). \quad (3.6)$$

Remark 3.2. *Because of the nesting property (3.2), a HPS spline can also be represented as a sum of $(l+1)$ PS splines $s^k(x,y)$, associated with each refinement level k in the hierarchical mesh, i.e.,*

$$s_H(x,y) = \sum_{k=0}^l s^k(x,y), \quad (3.7)$$

where the splines $s^k(x,y) \in S_2^1(\Delta^{*,k})$, as defined in Remark 3.1, are constrained to be zero outside the union of all triangulation patches in Δ_H of level k . These splines represent the detail added at each level. To form a compact hierarchical basis, we can select the PS B-splines of each $s^k(x,y)$ that are associated with newly introduced conforming vertices at level k in the hierarchical mesh.

In the next section, we consider the construction of a compact quasi-hierarchical basis for the spline space $S_{2,H}^1(\Delta_H^*)$. It results in the representation

$$s_H(x,y) = \sum_{i=1}^{n_c} \sum_{j=1}^3 c_{i,j} B_{i,QH}^j(x,y). \quad (3.8)$$

We shall call a hierarchical spline in its quasi-hierarchical representation (3.8) a QHPS spline.

3.2 A quasi-hierarchical Powell-Sabin spline basis

We associate with each conforming vertex V_i in the hierarchical mesh Δ_H three linearly independent basis functions $B_{i,QH}^j(x, y)$, $j = 1, 2, 3$, called QHPS B-splines.

Definition 3.1 (QHPS B-spline). *A QHPS B-spline $B_{i,QH}^j(x, y)$ associated with the conforming vertex V_i is defined as the unique solution to interpolation problem (3.4) with all $(f_k, f_{x,k}, f_{y,k}) = (0, 0, 0)$, except for $k = i$, where $(f_k, f_{x,k}, f_{y,k}) = (\alpha_{i,j}, \beta_{i,j}, \gamma_{i,j}) \neq (0, 0, 0)$.*

Figure 6 illustrates how a QHPS B-spline associated with the central vertex in the given triangulation changes when some of the triangles are triadically refined. In the example the same triplet $(\alpha_{i,j}, \beta_{i,j}, \gamma_{i,j})$ is used in the three cases. Because the B-splines are non-zero at a single conforming vertex, they will have a local support.

Property 3.1 (Local support). *Let k be the smallest level of all triangles in the hierarchical mesh Δ_H that contain the conforming vertex V_i . The QHPS B-spline $B_{i,QH}^j(x, y)$ is zero outside the molecule M_i^k of V_i in Δ_H^k .*

Proof. Consider the hierarchical triangulation $\tilde{\Delta}_H$ consisting of all triangles in Δ_H that lie outside the molecule M_i^k . Since the function values and gradients of $B_{i,QH}^j(x, y)$ at the conforming vertices in $\tilde{\Delta}_H$ are zero, the QHPS B-spline must be zero on $\tilde{\Delta}_H$ by Theorem 3.1. \square

In the next section we will see that the QHPS B-splines will form a convex partition of unity for some particular choices of $(\alpha_{i,j}, \beta_{i,j}, \gamma_{i,j})$.

Referring to Remark 3.1, a QHPS B-spline can be represented as a classical Powell-Sabin spline. The corresponding coefficients can be calculated by means of the following algorithm.

Algorithm 3.1 (Representation of a QHPS B-spline). *Let $B_{i,QH}^j(x, y)$ be a QHPS B-spline on the hierarchical mesh Δ_H with l refinement levels. The value, x - and y -derivative of $B_{i,QH}^j(x, y)$ at the conforming vertex V_i are equal to $\alpha_{i,j}$, $\beta_{i,j}$ and $\gamma_{i,j}$ respectively. The coefficients of the QHPS B-spline in representation (3.6) on Δ^l (with PS refinement $\Delta^{*,l}$) are computed as follows:*

1. *Let k be the smallest level of all triangles in Δ_H that contain the conforming vertex V_i . Denote $\Delta^{*,k}$ as the extended PS refinement of $\Delta_H^{*,k}$ (see Remark 3.1), and $\Delta^{*,k} \subseteq \Delta^{*,l}$ as the corresponding mesh structure. Calculate the control triangles of the PS spline (2.3) on $\Delta^{*,k}$ with value, x - and y -derivative at V_i equal to $\alpha_{i,j}$, $\beta_{i,j}$ and $\gamma_{i,j}$ respectively, and zero at the other vertices in Δ^k .*
2. *For m from $k + 1$ to l :*
 - (a) *Calculate the control triangles of the triadically subdivided PS spline on $\Delta^{*,m}$, using the subdivision rules (2.9).*
 - (b) *Set the values of the coefficients zero that correspond to conforming vertices in Δ_H^m different from V_i (and that are not zero yet).*
3. *The coefficients of the QHPS B-spline are the z -components of the control triangles.*

These coefficients are computed in a stable way, since Algorithm 3.1 only uses the PS subdivision rules which are convex combinations. One can intuitively verify that the algorithm constructs the desired B-spline as follows. During the iteration corresponding to level m , step 2b only changes the values of coefficients that are associated with vertices in the interior of a triangulation patch of level m in Δ_H^m . Since the remaining values are calculated by subdivision (step 2a), the spline will not be modified on the triangles in Δ_H of level $r < m$. It follows that the final spline is a quadratic polynomial on all triangles in Δ_H^* . Since this spline is also C^1 -continuous, it belongs to $S_{2,H}^1(\Delta_H^*)$. Step 1 and 2b ensures that the interpolation condition in Definition 3.1 is satisfied.

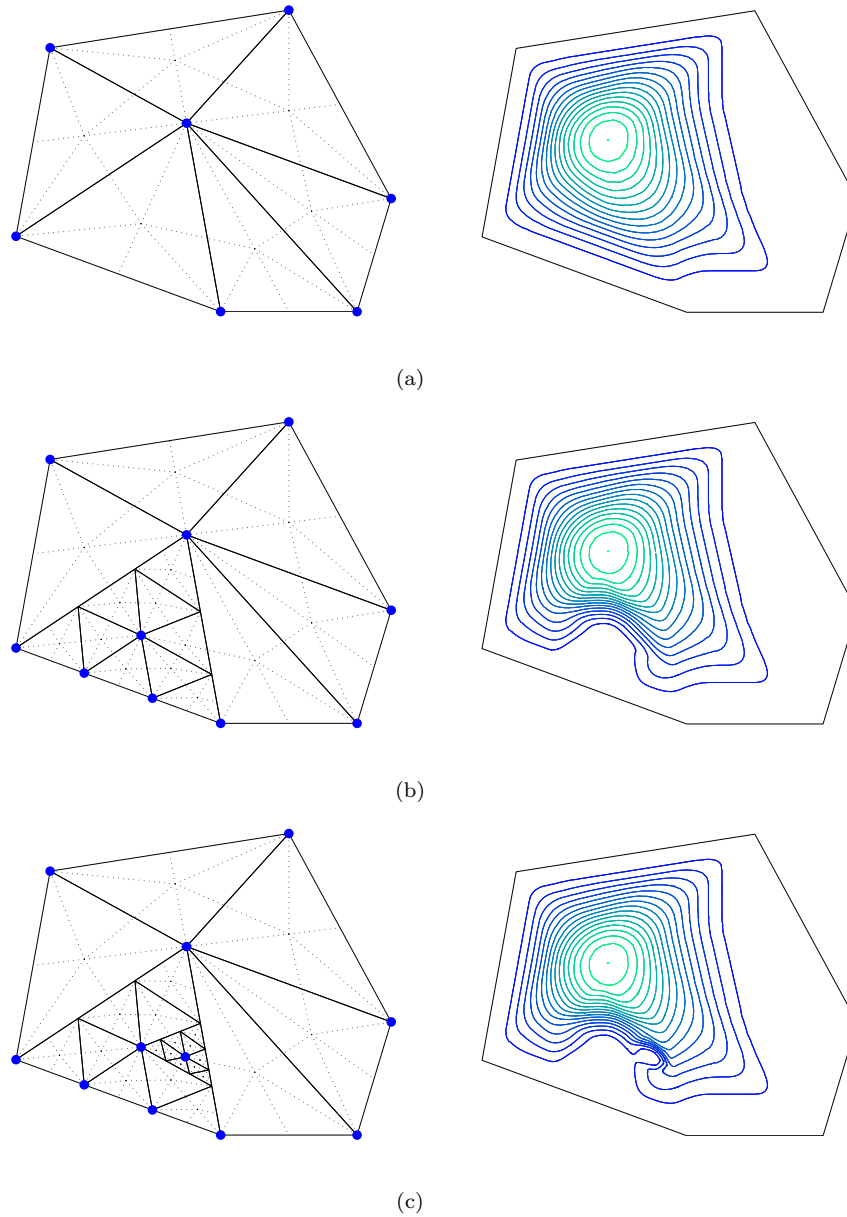


Figure 6: Contour plot of a QHPS B-spline (right) associated with the same vertex for several triadically refined meshes (left). The HPS refinement is indicated with dotted lines, and the conforming vertices with bullets. Each B-spline differs from zero at a single conforming vertex.

3.3 QHPS splines in a normalized B-spline basis

We will follow the common practice for the classical PS B-splines, and identify the three QHPS basis functions $B_{i,QH}^j(x, y)$ at the conforming vertex V_i by means of a QHPS triangle t_i . Such a QHPS basis will be a normalized basis in the sense that the B-splines form a convex partition of unity (1.2).

Definition 3.2 (QHPS point). Let k be the smallest level of all triangles in the hierarchical mesh Δ_H that contain the conforming vertex V_i . The QHPS points of V_i are the PS points of V_i in the PS refinement $\Delta^{*,k}$.

Definition 3.3 (QHPS triangle). A QHPS triangle t_i of vertex V_i is a triangle that contains all QHPS points of V_i .

Figure 4(b) depicts the QHPS points and suitable QHPS triangles for an example triangulation. From such a QHPS triangle we can determine the value and derivatives of the three corresponding QHPS B-splines at the considered vertex, using the relation (2.4). Further on, we shall always assume that the QHPS B-splines are defined by means of a set of QHPS triangles.

Lemma 3.1. Let $s_H(x, y) \in S_{2,H}^1(\Delta_H^*)$ be represented as a PS spline s^l in the form (3.6) and as a QHPS spline s_{QH} in the form (3.8). If the QHPS triangles of s_{QH} are used as the PS triangles of s^l , then $c_{i,j} = c_{i,j}^l$ for all conforming vertices V_i in Δ_H .

Proof. Note first that a QHPS triangle is a valid PS triangle for the extended PS refinement $\Delta^{*,l}$. Indeed, it contains the QHPS points which are situated further away from the vertex than the required PS points for a valid PS triangle on $\Delta^{*,l}$. If the QHPS triangles are used as PS triangles, then the value and gradient of the QHPS B-splines at the conforming vertices are equal to the ones of the PS B-splines, because of the common relation (2.4). Obviously, the value and gradient of the QHPS spline s_{QH} and its PS spline representation s^l are also identical at these vertices. These equalities can only be ensured as the coefficients of both splines, associated with the conforming vertices, are equal. \square

We will now prove that the considered QHPS B-splines form a convex partition of unity.

Property 3.2 (Positivity). The QHPS B-splines are positive.

Proof. The QHPS B-spline $B_{i,QH}^j(x, y)$ can be written as a linear combination of PS B-splines, i.e., $B_{i,QH}^j(x, y) = \sum_{u=1}^{n_i} \sum_{v=1}^3 b_{u,v}^l B_u^{v,l}(x, y)$, as in (3.6). We will calculate the coefficients $b_{u,v}^l$ via Algorithm 3.1. If we use the QHPS triangle of vertex V_i as PS triangle in step 1 of the algorithm, then the constructed PS spline on $\Delta^{*,k}$ has a single coefficient equal to 1, and the other coefficients equal to zero. The algorithm only uses convex combinations, so that the coefficients $b_{u,v}^l$ will be positive. Since the PS B-splines $B_u^{v,l}$ are also positive, the property is proved. \square

Property 3.3 (Partition of unity). The QHPS basis forms a partition of unity.

Proof. We consider the QHPS spline s_{QH} in representation (3.8) with all coefficients equal to 1, i.e., the sum of the QHPS B-splines. By relation (2.4) it follows that $s_{QH}(V_i) = \sum_{j=1}^3 \alpha_{i,j} = 1$, $\frac{\partial}{\partial x} s_{QH}(V_i) = \sum_{j=1}^3 \beta_{i,j} = 0$ and $\frac{\partial}{\partial y} s_{QH}(V_i) = \sum_{j=1}^3 \gamma_{i,j} = 0$ for all conforming vertices V_i . Using Theorem 3.1, s_{QH} must be identical to the unity function. \square

With each conforming vertex V_i one can associate three control points $C_{i,j}$, $j = 1, 2, 3$, and one control triangle $T_i(C_{i,1}, C_{i,2}, C_{i,3})$, in a similar way as for classical PS splines, i.e. (2.7). These control triangles satisfy the following property.

Property 3.4 (Control triangles). The control triangle T_i is tangent to the QHPS spline at the vertex V_i .

Proof. It follows from Lemma 3.1 that a QHPS control triangle is a valid PS control triangle in the PS spline representation (3.6) of the quasi-hierarchical spline. Since a PS control triangle is tangent to the surface at the considered vertex, the QHPS control triangle is tangent too. \square

Using these control triangles one can interactively change the shape of a given QHPS surface locally in a predictable way. From Properties 3.2 and 3.3 it follows that the QHPS surface (3.8) lies inside the convex hull of its control points $C_{i,j}$.

The coefficients $c_{i,j}^l$ in the PS spline representation (3.6) can be computed from the QHPS control triangles using PS subdivision via the following algorithm. It is a generalization of Algorithm 3.1.

Algorithm 3.2 (Representation of a QHPS spline). *Let $s_{QH}(x, y)$ be a QHPS spline on the hierarchical mesh Δ_H with l refinement levels, defined by the QHPS control triangles T_i , $i = 1, \dots, n_c$. The coefficients of the QHPS spline in representation (3.6) on Δ^l (with PS refinement $\Delta^{*,l}$) are computed as follows:*

1. Let \mathcal{V}^0 be the set of conforming vertices V_j that belong to a triangle of level 0 in Δ_H . Define s^0 as a Powell-Sabin spline on $\Delta^{*,0}$ with the PS control triangles associated with the vertices $V_j \in \mathcal{V}^0$ taken equal to the QHPS control triangles of s_{QH} at V_j , and with the other control triangles chosen arbitrarily.
2. For m from 1 to l :
 - (a) Calculate the control triangles of the triadically subdivided PS spline s^m on $\Delta^{*,m}$, using the subdivision rules (2.9).
 - (b) Let \mathcal{V}^m be the set of conforming vertices V_j where m is the smallest level of all triangles in Δ_H that contain V_j . Set the PS control triangles corresponding to these vertices V_j equal to their QHPS control triangles.
3. The coefficients of the QHPS spline are the z -components of the control triangles.

In step 1 of the algorithm we cannot directly select all PS control triangles as QHPS control triangles for the PS spline s^0 , since on the (coarse) mesh Δ^0 it is not guaranteed that the QHPS control triangles of the conforming vertices $V_j \notin \mathcal{V}^0$ are valid PS control triangles. Because the algorithm only uses convex combinations, all coefficients $c_{i,j}^l$ are computed in a stable way.

Remark 3.3. *Algorithm 3.2 generates a control triangle for each non-conforming vertex, using only convex combinations of the QHPS control points associated with two conforming vertices in the hierarchical mesh. These vertices form an edge on which the non-conforming vertex is situated.*

The non-conformity of a hierarchical mesh allows a local triadic refinement in a natural way. That is why QHPS splines can be easily locally subdivided, as contrasted with classical PS splines [21].

Property 3.5 (Local subdivision). *A QHPS spline $s_{QH}(x, y)$ can be locally subdivided on a given set of triangles using the triadic PS subdivision rules.*

Proof. The QHPS control triangles of the conforming vertices in the original mesh remain valid on the refined mesh. We now prove that the PS control triangles generated by Algorithm 3.2 for the new conforming vertices are valid QHPS control triangles if the rescaling step is omitted during the PS subdivision step. There are two types of newly introduced conforming vertices:

1. vertices that were non-conforming vertices in the original hierarchical mesh, and
2. new vertices, added inside a triangle.

Suppose that we want to refine a single triangle with refinement level k . If more triangles must be refined, then we can repeat the following reasoning for each of them separately. For the new vertex inside the original triangle, the six triangles that contain the vertex in the refined mesh are all of level $(k + 1)$. For the other new conforming vertices (of type 1), it is easy to see that the smallest level of all triangles containing such a vertex in the refined mesh must also be $(k + 1)$. Referring to Definition 3.3, the PS triangles of these vertices calculated in the $(k + 1)$ th iteration step of Algorithm 3.2 are valid QHPS triangles.

Since the control triangles generated by Algorithm 3.2 are obtained from the original QHPS control triangles, we have shown how the new QHPS control triangles can be computed via the PS subdivision rules. Of course, only a few (locally applied) steps of the algorithm are usually needed. \square

3.4 Stability of the QHPS basis

We specify stability for a hierarchical basis as in [3].

Definition 3.4 (Stability). *A hierarchical basis is weakly L_∞ -stable if the constants k_1^{-1} and k_2 in (2.6) have at most a polynomial growth in the number of levels. The basis is strongly L_∞ -stable if these constants are independent of the number of levels.*

The proof of the stability theorem will be similar to the one for classical Powell-Sabin splines [17]. However, our bound will be somewhat sharper. Denote $\theta_{\Delta_H^*}$ as the smallest angle in Δ_H^* , and let $|\rho|$ be the length of the longest edge of triangle ρ . We first introduce two lemmas.

Lemma 3.2. *Let $s_{QH}(x, y)$ be a QHPS spline defined on the HPS refinement Δ_H^* . Consider a triangle $\rho^* \in \Delta_H^*$, and denote its inradius as r_{ρ^*} . It holds that*

$$\left\| \frac{\partial}{\partial x} s_{QH} \right\|_{\infty, \rho^*} \leq \frac{12}{r_{\rho^*}} \|s_{QH}\|_{\infty, \rho^*}, \quad \text{and,} \quad \left\| \frac{\partial}{\partial y} s_{QH} \right\|_{\infty, \rho^*} \leq \frac{12}{r_{\rho^*}} \|s_{QH}\|_{\infty, \rho^*}, \quad (3.9)$$

with $\|\cdot\|_{\infty, \rho^*}$ the L_∞ -norm on ρ^* .

Proof. The relations (3.9) hold for the classical PS splines [17]. Since a QHPS spline is a PS spline when restricted on a single triangle, these relations are also valid for QHPS splines. \square

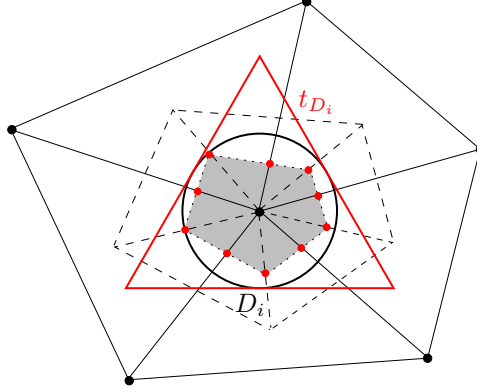
The following definition and lemma deal with the choice of the QHPS triangles. This choice will be important, since the B-splines and hence the approximation constants in (2.6) depend on these triangles. We introduce a constant K that reflects the size and shape of the QHPS triangles used in the definition of a normalized QHPS B-spline basis. One can always find a set of QHPS triangles that satisfy $K = 1$.

Definition 3.5. *Let D_i be the smallest disk with radius r_i and vertex V_i as center that contains all the QHPS points of V_i , as shown in Figure 7. For each conforming vertex V_i we define K_i as the smallest value such that there exists an equilateral triangle t_{D_i} with inradius $K_i r_i$ which contains the actual QHPS triangle t_i . Define K as the maximum of all constants K_i for each conforming vertex V_i in Δ_H .*

Lemma 3.3. *Let k be the smallest level of all triangles in the hierarchical mesh Δ_H that contain the conforming vertex V_i . Consider a triangle $\rho^{*,k} \in \Delta_H^*$ of level k that contains V_i , and denote by t_i the QHPS triangle of V_i . It holds that*

$$|t_i| \leq \sqrt{3} K_i L |\rho^{*,k}|, \quad (3.10)$$

with $L = \sin(\theta_{\Delta_H^*})^{-\pi/\theta_{\Delta_H^*}}$.

Figure 7: The disk D_i and the equilateral triangle t_{D_i} for $K_i = 1$.

Proof. Let l_1 and l_2 be the lengths of two sides of the same triangle ρ . By the law of sines it follows

$$\sin(\theta_\rho) l_1 \leq l_2 \leq |\rho|, \quad (3.11)$$

with θ_ρ the smallest angle in ρ . Using (3.11) we find that for any two triangles ρ_1 and ρ_2 in the same molecule M ,

$$\sin(\theta_M)^{\lfloor m/2 \rfloor} |\rho_1| \leq |\rho_2|, \quad (3.12)$$

with θ_M the smallest angle in the molecule, and m the number of triangles in the molecule. This number can be bounded by $m \leq 2\pi/\theta_M$.

In [17] it is shown that $|t_i| \leq \sqrt{3} K_i |\rho_m^{*,k}|$, where $\rho_m^{*,k} \in \Delta^{*,k}$ contains the PS point in $\Delta^{*,k}$ with the longest distance to vertex V_i . Since $\rho_m^{*,k}$ and $\rho_m^{*,k}$ both lie in the molecule of V_i in $\Delta^{*,k}$, it follows from (3.12) that $|\rho_m^{*,k}| \leq \sin(\theta_{\Delta_H^*})^{-\pi/\theta_{\Delta_H^*}} |\rho^{*,k}|$. \square

We now come to the main theorem of this section.

Theorem 3.2 (Stability). *The QHPS basis is strongly L_∞ -stable, i.e., for any coefficient vector c in the QHPS spline representation (3.8) we have*

$$k_1 \|c\|_\infty \leq \|s_{QH}(x, y)\|_\infty \leq k_2 \|c\|_\infty, \quad (3.13)$$

with

$$k_1 = \left(1 + \frac{48\sqrt{3}KL}{\tan(\theta_{\Delta_H^*}/2)} \right)^{-1}, \quad \text{and} \quad k_2 = 1. \quad (3.14)$$

Proof. The right inequality in (3.13) follows immediately from Properties 3.2 and 3.3. Using Property 3.4 and relation (2.4), we have for each conforming vertex V_i

$$\begin{bmatrix} s_{QH}(V_i) \\ \frac{\partial}{\partial x} s_{QH}(V_i) \\ \frac{\partial}{\partial y} s_{QH}(V_i) \end{bmatrix} = \begin{bmatrix} \alpha_{i,1} & \alpha_{i,2} & \alpha_{i,3} \\ \beta_{i,1} & \beta_{i,2} & \beta_{i,3} \\ \gamma_{i,1} & \gamma_{i,2} & \gamma_{i,3} \end{bmatrix} \begin{bmatrix} c_{i,1} \\ c_{i,2} \\ c_{i,3} \end{bmatrix} =: A_i c_i. \quad (3.15)$$

Taking into account that $\alpha_{i,3} = 1 - \alpha_{i,1} - \alpha_{i,2}$, $\beta_{i,3} = -\beta_{i,1} - \beta_{i,2}$ and $\gamma_{i,3} = -\gamma_{i,1} - \gamma_{i,2}$, we find that

$$A_i^{-1} = \begin{bmatrix} 1 & \eta_{i,1} & \mu_{i,1} \\ 1 & \eta_{i,2} & \mu_{i,2} \\ 1 & \eta_{i,3} & \mu_{i,3} \end{bmatrix}, \quad (3.16)$$

where (see [17])

$$\eta_{i,j} = (\alpha_{i,2}\gamma_{i,1} - \alpha_{i,1}\gamma_{i,2} + \delta_{j,1}\gamma_{i,2} - \delta_{j,2}\gamma_{i,1})/e, \quad (3.17a)$$

$$\mu_{i,j} = (\alpha_{i,1}\beta_{i,2} - \alpha_{i,2}\beta_{i,1} - \delta_{j,1}\beta_{i,2} + \delta_{j,2}\beta_{i,1})/e, \quad (3.17b)$$

with $\delta_{i,j}$ the Kronecker delta, and $e = \beta_{i,1}\gamma_{i,2} - \beta_{i,2}\gamma_{i,1}$. From [6] we know that $\beta_{i,j}$ and $\gamma_{i,j}$ can be written as

$$\beta_i = (\beta_{i,1}, \beta_{i,2}, \beta_{i,3}) = (Y_{i,2} - Y_{i,3}, Y_{i,3} - Y_{i,1}, Y_{i,1} - Y_{i,2})e, \quad (3.18a)$$

$$\gamma_i = (\gamma_{i,1}, \gamma_{i,2}, \gamma_{i,3}) = (X_{i,3} - X_{i,2}, X_{i,1} - X_{i,3}, X_{i,2} - X_{i,1})e. \quad (3.18b)$$

Combining the expressions (3.17) and (3.18), together with $\alpha_{i,j} \geq 0$, we obtain that

$$\begin{aligned} |\eta_{i,1}| &= |\alpha_{i,2}\gamma_{i,1} + (1 - \alpha_{i,1})\gamma_{i,2}|/|e| = |\alpha_{i,2}(X_{i,3} - X_{i,2}) + (\alpha_{i,2} + \alpha_{i,3})(X_{i,1} - X_{i,3})| \\ &= |\alpha_{i,2}(X_{i,1} - X_{i,2}) + \alpha_{i,3}(X_{i,1} - X_{i,3})| \leq \alpha_{i,2}|X_{i,1} - X_{i,2}| + \alpha_{i,3}|X_{i,1} - X_{i,3}| \\ &\leq (\alpha_{i,2} + \alpha_{i,3})|t_i| \leq |t_i|. \end{aligned}$$

Similarly we find that $|\eta_{i,j}|, |\mu_{i,j}| \leq |t_i|$, and in combination with Lemma 3.3, it results in

$$|\eta_{i,j}|, |\mu_{i,j}| \leq \sqrt{3} K_i L |\rho^{*,k}| \leq \sqrt{3} K L |\rho^{*,k}|, \quad (3.19)$$

for a triangle $\rho^{*,k} \in \Delta_H^*$ as defined in Lemma 3.3. Suppose that $\|c\|_\infty = |c_{i,j}|$. Then,

$$\|c\|_\infty = |s_{QH}(V_i) + \eta_{i,j} \frac{\partial}{\partial x} s_{QH}(V_i) + \mu_{i,j} \frac{\partial}{\partial y} s_{QH}(V_i)|. \quad (3.20)$$

Using Lemma 3.2 and inequality (3.19), we deduce that

$$\begin{aligned} \|c\|_\infty &\leq \|s_{QH}\|_{\infty, \rho^{*,k}} \left(1 + \frac{12(|\eta_{i,j}| + |\mu_{i,j}|)}{r_{\rho^{*,k}}} \right) \\ &\leq \|s_{QH}\|_{\infty, \rho^{*,k}} \left(1 + \frac{24\sqrt{3} K L |\rho^{*,k}|}{r_{\rho^{*,k}}} \right). \end{aligned} \quad (3.21)$$

The inradius r_ρ of a triangle ρ can be written as

$$r_\rho = \tan\left(\frac{\theta_3}{2}\right) \frac{l_1 + l_2 - l_3}{2}, \quad (3.22)$$

with l_i the lengths of the sides of ρ , and l_3 corresponds to the side opposite to angle θ_3 . Let θ_ρ be the smallest angle in ρ , then the inradius can be bounded below by

$$r_\rho \geq \tan\left(\frac{\theta_\rho}{2}\right) \frac{|\rho|}{2}. \quad (3.23)$$

Filling (3.23) into (3.21), we find that

$$\|c\|_\infty \leq \|s_{QH}\|_\infty \left(1 + \frac{48\sqrt{3} K L}{\tan(\theta_{\Delta_H^*}/2)} \right). \quad (3.24)$$

□

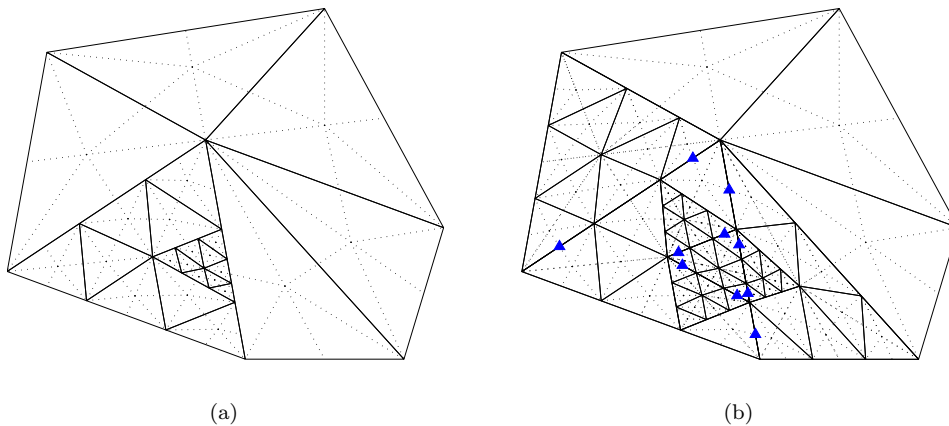


Figure 8: (a) A given hierarchical mesh. (b) The computed triangles for the construction of an extensible HPS refinement of the mesh in (a). These extensions of the local PS refinements at each level fix the positions of the points R_j at the boundary edges of the original refined regions that are not part of the boundary of the domain. The positions of these points are indicated with triangle symbols.

4 Practical implementation aspects

In this section we discuss some practical implementation issues. First, we explain how a HPS refinement can be constructed such that the hierarchical mesh can be locally triadically refined in an efficient way. Then, we show how algorithms for classical Powell-Sabin B-splines can be used for the quasi-hierarchical variant.

4.1 Practical construction of the hierarchical mesh

The (local) subdivision strategy must allow that new triangles can be easily refined at a certain level in the hierarchical mesh while preserving the edges in the original mesh and its HPS refinement. If one decides to refine the triangle ρ_l that is adjacent to the already refined triangle ρ_k , the new interior point Z_l of ρ_l must be collinear with two points, i.e. the interior point Z_k of ρ_k and the HPS refinement point R_j on the common edge. Otherwise, the new HPS refinement will not be valid.

To anticipate such a situation and to avoid its related problems, it is better not to choose the HPS refinement points R_j arbitrarily at the boundary of the triangulation patches of each refinement level. Instead, we suggest the following procedure. We will first determine the interior points Z_l of the neighbouring triangles before we fix the positions of the points R_j . To that end, for each refined triangle in the original mesh, we will also triadically split the adjacent triangles at the same refinement level. Then, we will build the HPS refinement on the extended set of triangles. For example, to construct an easily extensible HPS refinement of the mesh in Figure 6(c), we will select the HPS refinement points R_j as computed in the mesh of Figure 8. Note that we do not have to define the HPS refinement points at the boundary of the extended triangulation patches (see Figure 8), since they are not needed in the computation of the points R_j .

The extra computed triangles are only needed for the construction of the HPS refinement, and are not required for further calculations on the QHPS spline. Moreover, the number of these triangles is still limited, and they could be recovered in a further triadic refinement of the hierarchical mesh.

4.2 A generic algorithm for QHPS splines

Many efficient and stable algorithms exist for classical Powell-Sabin splines, e.g, to evaluate, to visualize, and to manipulate the splines. In this section we show how these algorithms can be used for working with quasi-hierarchical Powell-Sabin splines. A QHPS spline can be represented on each leaf triangle by a particular PS spline. To construct this PS spline, we have to determine the control triangles corresponding to the three corners of the considered triangle. The control triangles associated with conforming vertices can be taken identical to the control triangles of the QHPS spline. As mentioned in Remark 3.3, we can use subdivision to obtain the control triangles for non-conforming vertices. The correct values can be easily computed while moving up in the hierarchical mesh structure. Then, when the leaf triangle is reached, the corresponding PS spline on the considered triangle will be fully defined. In this way, an algorithm for QHPS splines can be straightforwardly reduced to the equivalent algorithm for PS splines. The generic QHPS algorithm looks as follows:

Algorithm 4.1. *Let Δ_H be a hierarchical mesh structure, and Δ be a conforming mesh. The generic algorithm `qhps_algorithm(Δ_H)` for QHPS splines is based on the equivalent algorithm `ps_algorithm(Δ)` for classical PS splines.*

```

function qhps_algorithm(hierarchical_structure  $\Delta_H$ )
  for all triangles  $\rho$  in the initial triangulation  $\Delta^0$  of  $\Delta_H$ :
    qhps_local_algorithm( $\rho$ ,  $\Delta_H$ )
  endfor
end

function qhps_local_algorithm(triangle  $\rho$ , hierarchical_structure  $\Delta_H$ )
  if  $\rho$  is not a leaf triangle:
    1. Let  $l$  be the level of  $\rho$  in the hierarchical structure.
    2. for all non-conforming vertices  $V_i$  of level  $(l + 1)$  at the interior of an edge of  $\rho$ :
      Calculate the control triangle  $T_i$  by PS subdivision, using the control triangles
      of two corner vertices of  $\rho$ .
    endfor
    3. for all 9 subtriangles  $\rho_i$  of level  $(l + 1)$  in  $\rho$ :
      qhps_local_algorithm( $\rho_i$ ,  $\Delta_H$ )
    endfor
  else
    ps_algorithm( $\rho$ )
  endif
end

```

Remark 4.1. *Using a different Powell-Sabin spline on each leaf triangle in the hierarchical mesh is usually not more time-consuming than considering one PS spline per triangulation patch. Indeed, most of the algorithms for PS splines run over all triangles in the mesh separately.*

Remark 4.2. *The QHPS splines can be evaluated and manipulated in a stable way. Only convex combinations are needed to convert the QHPS spline on each triangle to a PS spline, to represent these PS splines with Bernstein-Bézier polynomials, and to evaluate these polynomials via the de Casteljau algorithm.*

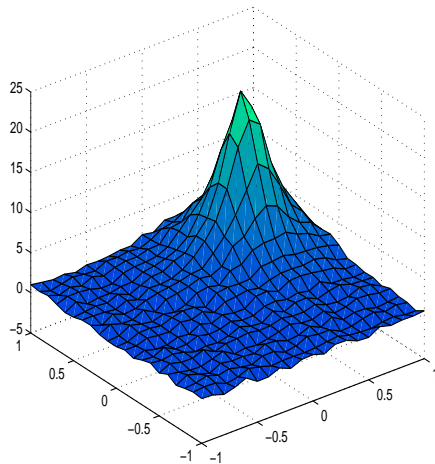


Figure 9: Noisy data values of the function $(\exp((x - 0.52)^2 + (y - 0.48)^2) - 0.95)^{-1}$.

5 Applications

In this section we consider two applications of quasi-hierarchical Powell-Sabin splines: smoothing noisy measurement data, and surface modelling.

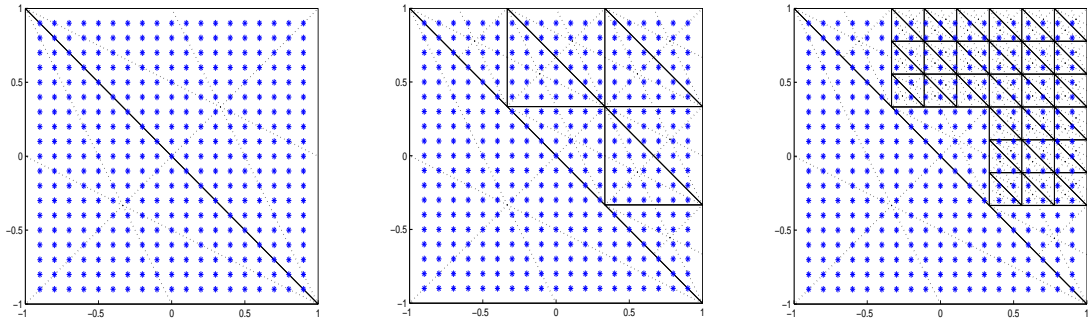
5.1 Data fitting

Given a set of data points p_r , $r = 1, \dots, m$, with corresponding (noisy) data values f_r . We wish to determine a spline that approximates the underlying smooth function. In this example, we use the least squares criterion, i.e., we determine the spline s_{QH} such that

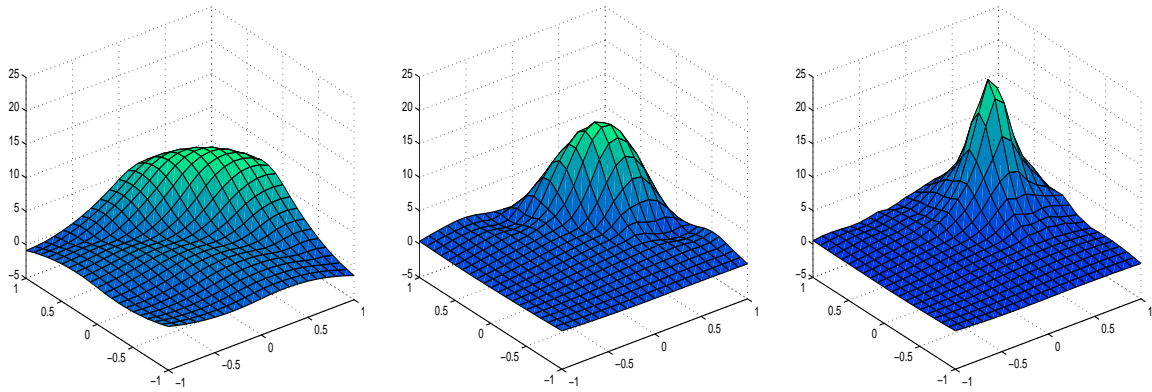
$$\sum_{r=1}^m (f_r - s_{QH}(p_r))^2 \quad (5.1)$$

is minimized. As example we consider the test function $(\exp((x - 0.52)^2 + (y - 0.48)^2) - 0.95)^{-1}$, taken from [7]. The data values, sampled on a regular grid, are perturbed by normally distributed noise with zero expected value and standard deviation equal to 0.25. The noisy data interpolant is shown in Figure 9. The following simple adaptive strategy has been implemented. For more advanced methods we refer to [7, 5]. We start with a regular conforming triangulation consisting of 2 triangles. Then, the triangles with the largest sum of squared weighted residuals are refined till the solution is considered satisfactory (see Figure 10). Since the original spline space is a subspace of the refined one, we are guaranteed of a better approximation with an increased local resolution. For the QHPS spline approximation in Figure 10(b) on the finest mesh, there are 3×33 degrees of freedom.

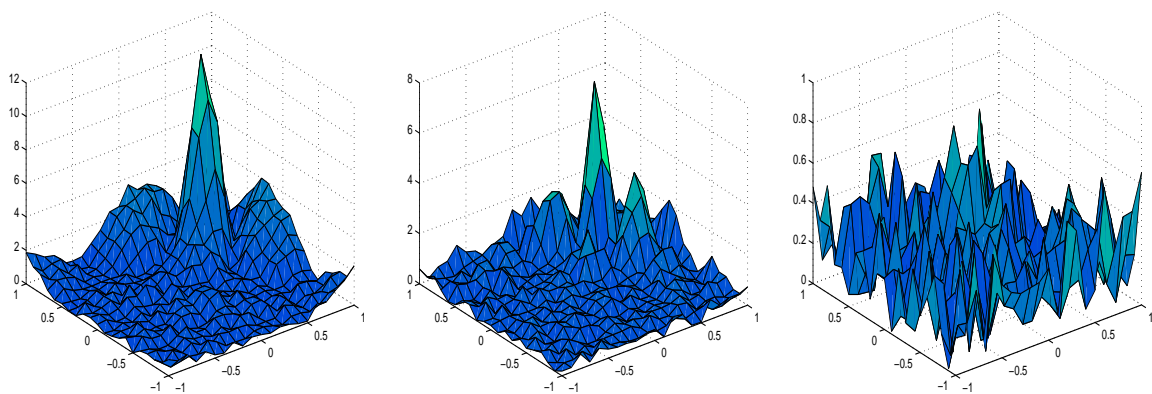
Remark 5.1. *The results globally depend on the data values, in contrast to a method that would progressively reduce the residuals by adding constrained PS splines on the locally refined triangulation patch. The values of the coefficients associated with vertices outside the refined patch also change as the refinement proceeds. For example, the values of the three coefficients corresponding to vertex $V_i(-1, -1)$ in Figure 10(b) vary as $(-2.22, 1.22, 5.83)$, $(0.08, 0.45, 2.00)$ and $(0.05, 0.39, 2.09)$ for the three different meshes. The corresponding spline values $s_{QH}(V_i)$ are 1.61, 0.84 and 0.84*



(a) Triangulations with the positions of the data points



(b) Approximating uniform QHPS spline interpolants



(c) Approximation errors

Figure 10: Smoothing uniform QHPS spline approximations of the noisy data values in Figure 9, for different refinement levels.

respectively. Of course, the further the vertices are away from the refined patch, the less their coefficients change.

Remark 5.2. *When the initial mesh consists of identical triangles, as in Figure 10(a), all triangles in the refined meshes will be uniform. We will call the corresponding spline a uniform QHPS spline. Due to the high degree of symmetry, the HPS refinement is known in advance, and the shape of the QHPS triangles can be fixed, i.e., for vertex $V_i(x, y)$ the corners of the QHPS triangle are*

$$Q_{i,1}(x + h/2, y), \quad Q_{i,2}(x - h/2, y + h/2), \quad \text{and} \quad Q_{i,3}(x, y - h/2), \quad (5.2)$$

with h the largest local mesh size. Thus, the calculation of suitable QHPS triangles containing the QHPS points at each vertex is no longer required. This enables us to implement the uniform QHPS algorithms more efficiently.

5.2 Surface modelling

Local subdivision results in an efficient time and memory usage for representing complex surfaces. The new basis functions after subdivision have a smaller support and give the designer more local control for manipulating the surface. The locality of the subdivision scheme ensures that the dimension of the subdivided space stays reasonable.

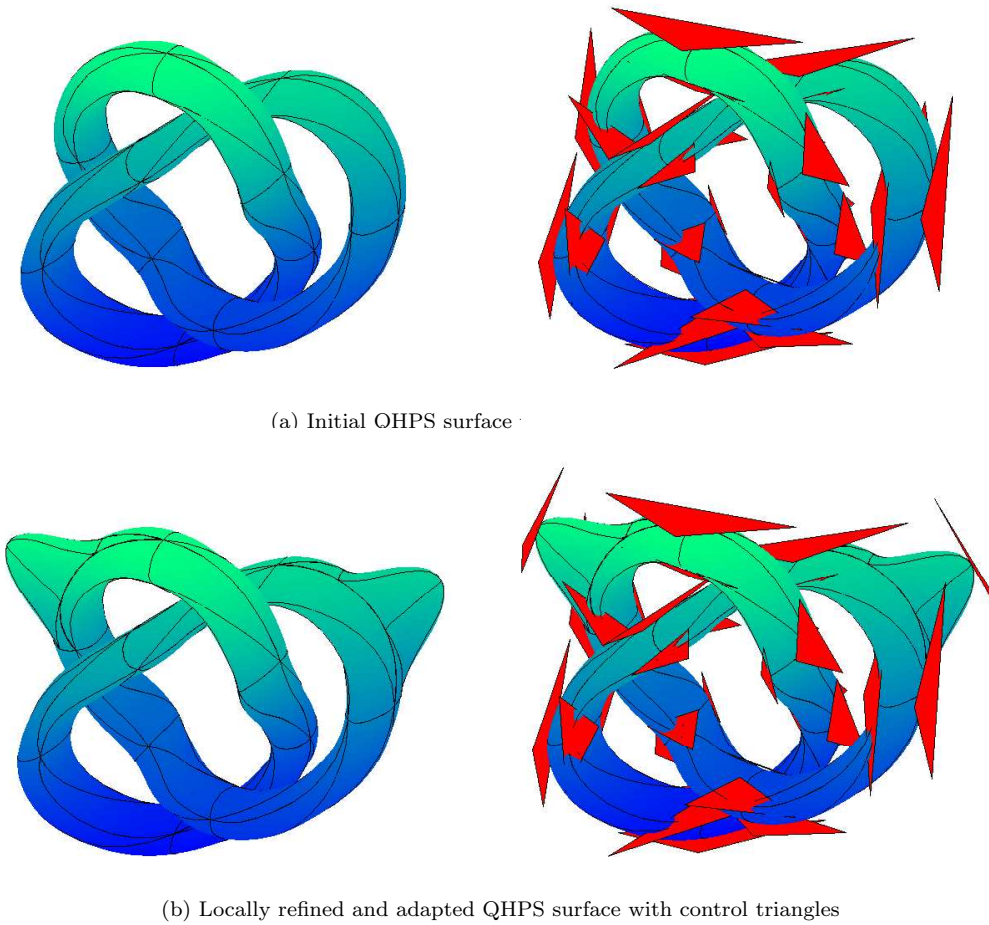
In the next example, we modelled the trefoil knot, using a parametric QHPS surface with 33 vertices. The QHPS splines defined in this paper can be easily extended to parametric surfaces. Such surfaces are defined by control points $C_{i,j} = (c_{i,j}^x, c_{i,j}^y, c_{i,j}^z)$, i.e., the coefficients of three QHPS splines, similar to parametric PS surfaces (see, e.g., [26, 21]). In Figure 11(a) the spline surface is depicted, together with its control triangles. We subdivided two triangles, and moved the control triangles of the newly introduced vertices, see Figure 11(b). The support of the B-splines associated with these new vertices stays within the original triangles. This property is very useful for surface editing: the user selects a triangle, where the surface can be locally subdivided, and then one can morph the surface such that only the part within the selected triangle is affected. The new QHPS surface only consists of 35 control triangles, whereas a globally subdivided Powell-Sabin surface would need 297 control triangles.

6 Concluding remarks

In this paper we presented hierarchical Powell-Sabin splines in a quasi-hierarchical representation. They are C^1 -continuous quadratic splines defined on a hierarchical triangulation, which can be non-conforming. Such a mesh is obtained, starting from a conforming triangulation, by partitioning successively a subset of triangles with a triadic split. The construction of the spline is based on a particular HPS refinement of the mesh, and the dimension of this spline space is equal to three times the number of conforming vertices in the mesh.

Instead of the triadic refinement scheme, other schemes could be used as well. For instance, one can apply the dyadic scheme from [26] for uniform PS splines, that splits each triangle into four subtriangles. However, the dyadic refinement of a single triangle is not able to create new degrees of freedom as in the triadic case, since only non-conforming vertices are introduced. Therefore, more triangles must be refined, e.g., all triangles in the molecule of a vertex.

We constructed a QHPS basis that retains all the advantages of the classical Powell-Sabin B-splines: the basis functions have a local support, they form a convex partition of unity, they are strongly L_∞ -stable, and the spline is locally controllable by means of control triangles. In addition, local subdivision can now be applied straightforwardly, since the mesh is no longer restricted to be



(a) Initial QHPS surface

(b) Locally refined and adapted QHPS surface with control triangles

Figure 11: (a) A trefoil knot modelled by a QHPS surface. The control triangles and the triangular mesh lines are shown. (b) Effect of moving some control triangles of the locally refined QHPS surface.

conforming. Local subdivision is of interest in many application domains. We considered in the paper data fitting and surface modelling.

We showed how the QHPS spline can be represented on each triangle by a classical PS spline. That allows us to apply existing efficient algorithms for PS splines to QHPS splines. When it is possible to work with uniform QHPS splines, the construction of the splines can be simplified even more.

Acknowledgement

Hendrik Speleers is funded as a Research Assistant of the Fund for Scientific Research Flanders (Belgium).

References

- [1] P. Alfeld and L.L. Schumaker. Smooth macro-elements based on Powell-Sabin triangle splits. *Adv. Comp. Math.*, 16:29–46, 2002.
- [2] J.H. Bramble, J.E. Pasciak, and J. Xu. Parallel multilevel preconditioners. *Math. Comp.*, 55:1–22, 1990.
- [3] M. Dæhlen, T. Lyche, K. Mørken, R. Schneider, and H.P. Seidel. Multiresolution analysis over triangles, based on quadratic Hermite interpolation. *J. Comput. Appl. Math.*, 119:97–114, 2000.
- [4] J. Deng, F. Chen, and Y. Feng. Dimensions of spline spaces over T-meshes. *J. Comput. Appl. Math.*, 194(2):267–283, 2006.
- [5] P. Dierckx. *Curve and Surface Fitting with Splines*. Oxford University Press, Oxford, 1993.
- [6] P. Dierckx. On calculating normalized Powell-Sabin B-splines. *Comput. Aided Geom. Design*, 15(1):61–78, 1997.
- [7] P. Dierckx, S. Van Leemput, and T. Vermeire. Algorithms for surface fitting using Powell-Sabin splines. *IMA J. Numer. Anal.*, 12:271–299, 1992.
- [8] G. Farin. Triangular Bernstein-Bézier patches. *Comput. Aided Geom. Design*, 3(2):83–127, 1986.
- [9] G. Farin. *Curves and Surfaces for CAGD: A Practical Guide*. Morgan Kaufmann Publishers, San Francisco, fifth edition, 2002.
- [10] D.R. Forsey and R.H. Bartels. Hierarchical B-spline refinement. *Computer Graphics*, 22(3):205–212, 1988.
- [11] D.R. Forsey and R.H. Bartels. Surface fitting with hierarchical splines. *ACM Trans. Graphics*, 14(2):134–161, 1995.
- [12] E. Grinspun, P. Krysl, and P. Schröder. CHARMS: a simple framework for adaptive simulation. *ACM Trans. Graphics*, 21(3):281–290, 2002.
- [13] B. Jawerth and W. Sweldens. An overview of wavelet based multiresolution analyses. *SIAM Review*, (3):377–412, 1994.
- [14] R. Kraft. Adaptive and linearly independent multilevel B-splines. In A.L. Méhauté, C. Rabut, and L.L. Schumaker, editors, *Surface Fitting and Multiresolution Methods*, pages 209–218, Nashville, 1998. Vanderbilt University Press.
- [15] P. Krysl, E. Grinspun, and P. Schröder. Natural hierarchical refinement for finite element methods. *Int. J. Numer. meth. Eng.*, 56(8):1109–1124, 2003.
- [16] M.J. Lai and L.L. Schumaker. Macro-elements and stable local bases for spaces of splines on Powell-Sabin triangulations. *Math. Comp.*, 72:335–354, 2003.
- [17] J. Maes, E. Vanraes, P. Dierckx, and A. Bultheel. On the Stability of normalized Powell-Sabin B-splines. *J. Comput. Appl. Math.*, 170(1):181–196, 2004.
- [18] M.J.D. Powell and M.A. Sabin. Piecewise quadratic approximations on triangles. *ACM Trans. Math. Softw.*, 3:316–325, 1977.
- [19] T.W. Sederberg, D.L. Cardon, G.T. Finnigan, N.S. North, J. Zheng, and T. Lyche. T-spline simplification and local refinement. *ACM Trans. Graphics*, 23(3):276–283, 2004.

- [20] T.W. Sederberg, J. Zheng, A. Bakenov, and A. Nasri. T-splines and T-NURCCs. *ACM Trans. Graphics*, 22(3):161–172, 2003.
- [21] H. Speleers, P. Dierckx, and S. Vandewalle. Local subdivision of Powell-Sabin splines. *Comput. Aided Geom. Design*, 23(5):446–462, 2006.
- [22] H. Speleers, P. Dierckx, and S. Vandewalle. Numerical solution of partial differential equations with Powell-Sabin splines. *J. Comput. Appl. Math.*, 189(1-2):643–659, 2006.
- [23] E. Vanraes, J. Maes, and A. Bultheel. Powell-Sabin spline wavelets. *Int. J. Wav. Multires. Inf. Proc.*, 2(1):23–42, 2004.
- [24] E. Vanraes, J. Windmolders, A. Bultheel, and P. Dierckx. Automatic construction of control triangles for subdivided Powell-Sabin splines. *Comput. Aided Geom. Design*, 21(7):671–682, 2004.
- [25] F. Weller and H. Hagen. Tensor-product spline spaces with knot segments. In M. Dæhlen, T. Lyche, and L.L. Schumaker, editors, *Mathematical Methods for Curves and Surfaces*, pages 563–572, Nashville, 1995. Vanderbilt University Press.
- [26] J. Windmolders and P. Dierckx. Subdivision of uniform Powell-Sabin splines. *Comput. Aided Geom. Design*, 16:301–315, 1999.
- [27] H. Yserentant. On the multilevel splitting of finite element spaces. *Numer. Math.*, 49:379–412, 1986.